Transient Polymers through Carbodiimide-driven Assembly

Nirob K. Saha, William S. Salvia, Dominik Konkolewicz*, and C. Scott Hartley*

*Correspondence: DK: d.konkolewicz@miamioh.edu, CSH: scott.hartley@miamioh.edu

Department of Chemistry and Biochemistry, Miami University, 651 E High St, Oxford, OH, 45056, United States

Abstract: Biochemical systems make use of out-of-equilibrium polymers generated under kinetic control. Inspired by these systems, many abiotic supramolecular polymers driven by chemical fuel reactions have been reported. Conversely, polymers based on transient covalent bonds have received little attention, even though they have the potential to complement supramolecular systems by generating transient structures based on stronger bonds and by offering a straightforward tuning of reaction kinetics. In this study, we show that simple aqueous dicarboxylic acids give poly(anhydrides) when treated with the carbodiimide EDC. Transient covalent polymers with molecular weights exceeding 15,000 are generated which then decompose over the course of days. Disassembly kinetics can be controlled using simple substituent effects in the monomer design. The impact of solvent polarity, carbodiimide concentration, and monomer concentration on polymer properties and lifetimes has been investigated. The results reveal substantial control over polymer assembly and disassembly kinetics, highlighting the potential for fine-tuned kinetic control in nonequilibrium polymerization systems.

Introduction

Biology makes frequent use of out-of-equilibrium chemical reaction networks to regulate function. These systems offer temporally controlled, responsive behavior that is not possible otherwise. Accordingly, the design of abiotic systems that replicate aspects of these reaction networks is of significant interest.[1–3] Recent reports include chemically driven molecular motors,[4,5] conformational changes,[6] macrocycle assembly,[7] molecular ratchets,[8] supramolecular gels,[1,9–15] molecular switches,[16] and polymer networks.[17–20] These active systems are generally driven out of equilibrium by a coupled chemical reaction, a “fuel” reaction, that leads to the formation of a simple transient bond.[21] Function arises when activation by the fuel reaction generates a transient species that ultimately returns to the initial, or “resting”, state. Various types of fuel reactions have been used in these systems, including biology’s choice, ATP hydrolysis;[22] simple alkylation using reactive alkyl halides;[9,23] transient protonation;[5,24] and carbodiimide hydration.[10,25]

Transient polymers, such as actin networks and microtubules, are a favored class of nonequilibrium species in nature.[26] They exhibit time-dependent structures governed by the kinetics of fuel consumption instead of thermodynamic stability.[27,28] This kinetic control leads to remarkable behavior such as temporally controlled fibril formation and collective motion. While abiotic systems do not yet capture the complexity of these systems,[29] there are numerous examples of abiotic supramolecular polymers generated through reaction networks.[14,30–32] Some examples add elements of more-sophisticated kinetic control. Notably, Das has developed self-assembled transient gels[33] and fibers[34] that make use of strategically placed catalytic sites to control the rate of disassembly. This work represents a significant step toward achieving more-nuanced control over the kinetics of covalent polymer formation and disassembly. Nevertheless, fine-grained kinetic control over these supramolecular systems is challenging as assembly and disassembly are generally fast compared to the (covalent) activation and deactivation reactions.

The assembly of transient *covalent* polymers would offer new opportunities for kinetic control of polymerization as both activation and deactivation rates could be controlled through well-understood chemical reaction kinetics. Further, covalent polymers would allow assembly and disassembly to be studied by different experimental methods, such as gel-permeation chromatography (GPC). Polymer networks with transient covalent crosslinks are now reasonably well known.[17–20] There have, however, been no reports of transient covalent linear polymers that would allow assembly and disassembly mechanisms to be studied, other than a few reports of polymeric byproducts of other processes. For example, earlier work from our group described the formation of PEG-like polymers in competition with the production of transient crown ethers.[25] The Boekhoven group reported the creation of transient oligomers of isophthalic acid[35] as part of the generation of dynamic combinatorial libraries. We have also obtained polymers as part of investigations of transient assembly of shape-persistent macrocycles.[7]

The transient assembly of even simple, soluble polymers remains unexplored, leaving key questions unanswered about kinetic control both through structure–property effects and reaction conditions. Here, we present the formation of transient polymers by dynamically assembling isomeric oligo(ethylene glycol) diacid monomers **mDA** and **pDA** into polymers **mP** and **pP**, respectively, as shown in Scheme 1. The transient bonds are generated by coupling carbodiimide hydration to the formation of hydrolytically unstable carboxylic anhydrides. This approach, first reported by Boekhoven followed by us in 2017,[10,25] has been used in a wide variety of nonequilibrium systems, including the assembly of transient gels,[15,36] droplets,[37,38] vesicles,[39] and polymer networks[40,41] and the operation of molecular motors.[4,8] We show that transient polymers with weight-averaged molecular weights (M_w) in excess of 15,000 can be generated through the treatment of diacid precursors with the carbodiimide EDC, with subsequent polymer decomposition through hydrolysis. The maximum molecular weights and lifetimes of the polymers can be regulated using solvent polarity and the concentrations of both carbodiimide and monomer. We show that simple substituent effects provide substantial control over polymer lifetime. Consequently, polymers of this type should provide a basis for more sophisticated approaches to kinetically controlled assembly, complementing existing supramolecular systems.

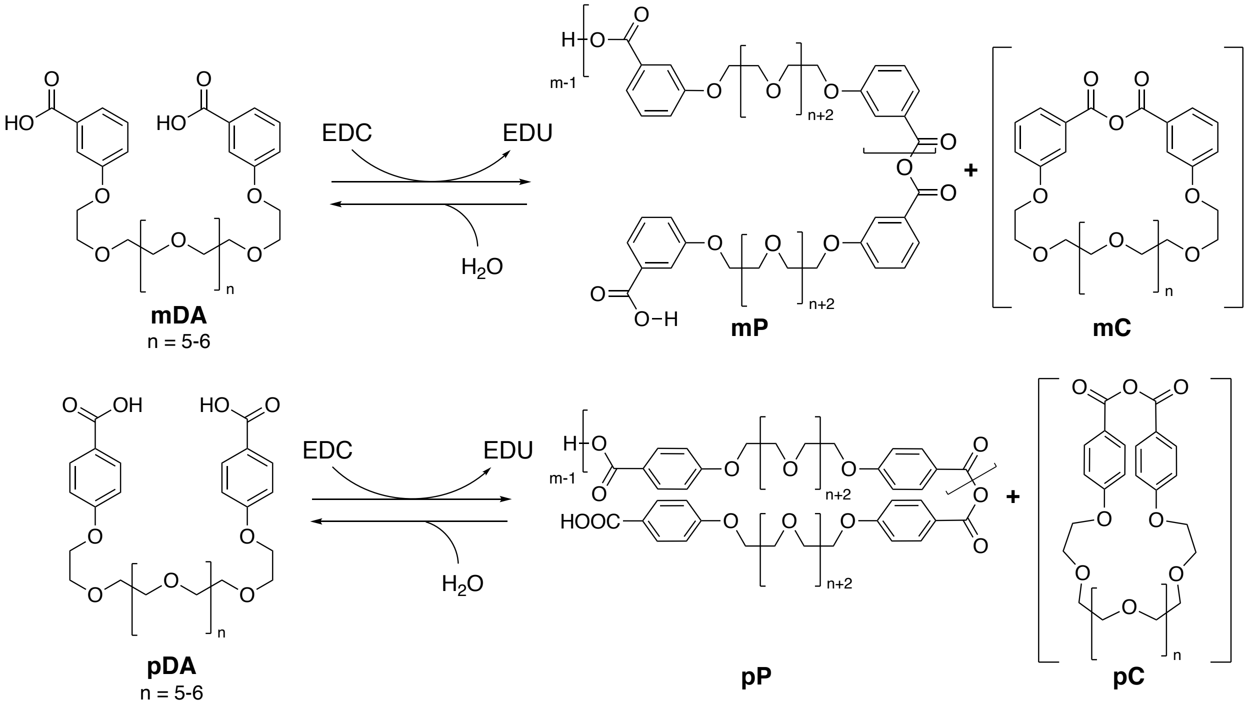

Scheme 1: Assembly of polymers **mP** and **pP** fueled by EDC.

Results and Discussion

Meta and para diacid monomers **mDA** and **pDA** are themselves short polymers, synthesized from a short PEG precursor (PEG-400) as described in the Supporting Information. The M_w of **mDA** and **pDA** were determined by GPC to both be 1000, with narrow dispersities ($Đ$) of 1.05 and 1.06, respectively. Both **mDA** and **pDA** are, unfortunately, insoluble in pure water. To minimize unwanted complexities from phase separation, acetone–water mixtures were therefore used throughout this study to ensure homogeneity throughout each experiment. We tested the behavior of both monomers on treatment with EDC at different ratios of acetone and water to identify suitable solvent compositions. Reaction mixtures from **mDA** generally remain homogeneous with higher proportions of water, with the products remaining soluble down to 60% acetone. In contrast, **pDA** reaction mixtures require at least 80% acetone to maintain solubility.

To compare the transient polymerization of monomers **mDA** and **pDA** (100 mM), each was dissolved in 80:20 acetone:water at room temperature and treated with one equivalent of EDC. Pyridine (40 mM) was included as an additive to minimize the formation of unwanted *N*-acylurea byproducts.[42] The progress of polymerization was monitored by GPC, as shown in Figure 1. Within minutes, both **mDA** and **pDA** formed polymers because of anhydride bond formation, with similar molecular weight distributions. In both cases, the maximum polymer length was reached in about 1 h. Concurrently, peaks at a lower apparent molecular weight than those of the original monomers appeared that were assigned to the formation of macrocycles **mC** and **pC** as side-products of polymerization.[43] The amount of **mC** and **pC** formed tended to be comparatively low, and within the reproducibility of the experiments it was not possible to say whether either system was more prone to cyclization.

Once generated, polymers **mP** and **pP,** as well as macrocycles **mC** and **pC,** then decomposed over the course of days at room temperature through anhydride bond hydrolysis. Notably, **pP** persisted much longer than **pM**.

The system was also studied by ^{1}H NMR spectroscopy. During the polymerization of **pDA**, two characteristic signals emerged at 8.07 and 7.13 ppm (Figure S19) indicative of the formation of both **pP** and **pC**, which could not be distinguished. Simultaneously, two signals at 7.94 and 7.03 ppm assigned to **pDA** disappeared. Near-complete consumption of **pDA** occurred within 0.5 h, coinciding with the transformation of the fuel EDC into EDU. Similarly, in the polymerization of **mDA**, new signals for **mP** and **mC** appeared (Figure S20), albeit overlapping with the aromatic proton signals of **mDA**. The consumption of the fuel was observed within the same 0.5 hour timeframe. ^{1}H NMR analysis (Figure S19 and S20) also indicated that the pyridine successfully minimized the formation of *N*-acylurea byproducts.[25,44]

To quantify the polymer properties, the GPC data were deconvoluted using a previously established protocol[45,46] and the results used to divide the chromatograms into separate contributions from macrocycle (**mC** and **pC)** and polymer (**mP** and **pP)** (see SI for details). The deconvoluted data enabled the calculation of number-averaged molecular weight (M_n), M_w, and $Đ$ of the polymers as a function of time. During the activation stage of the reaction cycle, both M_w and M_n of the polymers increased (Figure 1b, Figure S5). For **mP**, the highest M_w over the course of the experiment was 11,000 with $Đ$ of 1.95. Similarly, for **pP**, the highest M_w was 12,000 with $Đ$ of 1.94. The significant change in dispersity from ~1.05 (monomers **mDA** and **pDA**) to ~1.95 (polymers **mP** and **pP**) as the reactions progressed suggests a step-growth process, consistent with the EDC-fueled mechanism of anhydride bond formation of the diacid monomers. Note that as GPC analysis gives apparent rather than absolute molecular weights, the GPC data itself is subject to errors in the order of 10%,[47] with deconvolution leading to increased uncertainty**.**

The transient polymer lifetime (τ_{tpl}) is defined here as the time needed to dissipate 90% of the total transient polymer. From the deconvoluted GPC data, τ_{tpl} of the meta-diacid-based polymer **mP** is estimated at 7 d, whereas τ_{tpl} of the para-diacid-based polymer **pP** is estimated at >111 d. The slower hydrolysis of **pP** compared to **mP** is expected based on Hammett substituent constants,[48] and is consistent with previous work on similar acids.[49] For example, the hydrolysis rate of *meta*-methoxybenzoic anhydride is tenfold higher than that of *para*-methoxybenzoic anhydride, albeit under different conditions (58.25 °C, 75:25 dioxane:water).[50]

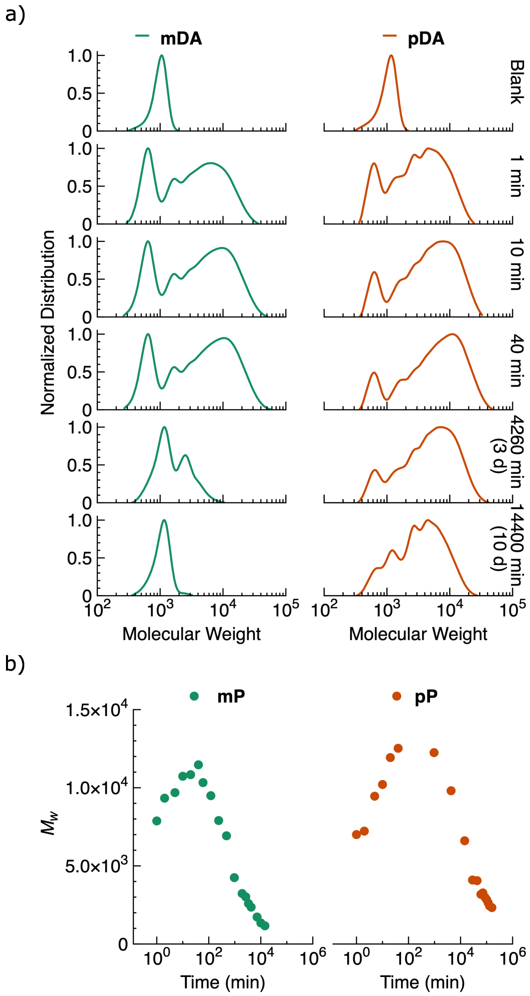

Figure 1: a) GPC chromatograms for the reaction of **mDA** (100 mM), EDC (100 mM), and pyridine (44 mM) and the reaction of **pDA** (100 mM), EDC (104 mM), and pyridine (42 mM) in 80:20 acetone:water at room temperature. b) Variation of M_w (determined from deconvolution of GPC data) for **mP** and **pP** against reaction time.

The impact of reaction conditions on the polymerization was studied for **mDA** since the timescale of its hydrolysis was more convenient and it tolerated higher proportions of water. Figure 2 shows the effect of varying solvent polarity on polymerization. Perhaps surprisingly, as the proportion of water increases there is a notable increase in the maximum molecular weight attained for the transient polymers. For instance, the largest M_w when using 80:20 acetone:water was 11,000 with $Đ$ of 1.95, while with 60:40 acetone:water the largest M_w was 16,000 with $Đ$ of 1.85. More-polar solvents appear to enhance the yield of the polymer by promoting productive anhydride formation over unproductive hydrolysis from the EDC-activated intermediate (e.g., *O*-acylisourea).

As expected, the hydrolysis rate of the anhydride-linked polymer was enhanced with higher water content in the system. The lifetime τ_{tpl} for transient polymer degradation was ~7 d for 80:20 acetone:water and ~1 d for 60:40 acetone:water. The increased decomposition rate was expected because of both the increased concentration of water and the increased solvent polarity, stabilizing charged intermediates, consistent with hydrolysis data for acetic anhydride in acetone–water mixtures.[51,52] Although the overall polymer lifetimes are still fairly long, these results demonstrate that solvent effects give substantial control over polymer (dis)assembly kinetics.

As expected, polymerization can be refueled through the addition of additional EDC after hydrolysis, as described in the Supporting Information (Figure S16). The behavior the second cycle is similar to the first, although the maximum polymer length is shorter and hydrolysis is somewhat faster. The difference could be due to interference from the EDU urea byproduct of the first cycle.

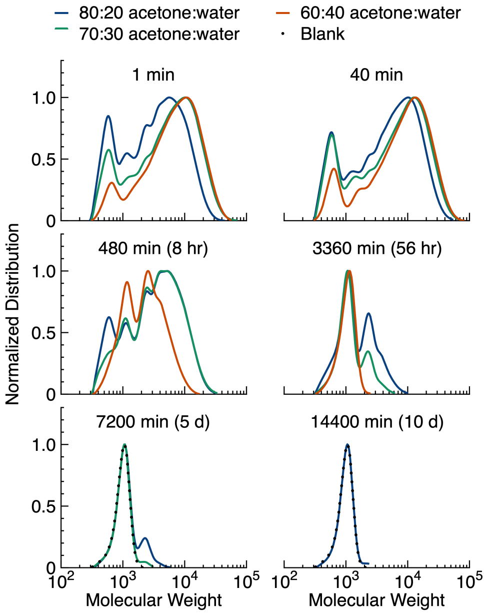

Figure 2: GPC chromatograms for polymerization of **mDA** with different ratios of acetone:water at room temperature. Conditions: mDA (101 mM), EDC (102 mM), and pyridine (63 mM) in 80:20 acetone:water; **mDA** (101 mM), EDC (102 mM), and pyridine (67 mM) in 70:30 acetone:water; and **mDA** (101 mM), EDC (101 mM), and pyridine (61 mM) in 60:40 acetone:water. 60:40 and 70:30 acetone:water are not included in the later plots as hydrolysis had already completed.

A hallmark of chemically driven transient assembly is that the outcome, notably the degree of assembly and the lifetime, is dictated by the fuel concentration. Figure 3 shows the effects of three different initial EDC concentrations on the **mDA** (101 mM) system. Changing from 0.5 to 1.0 equiv of EDC gives a substantial increase in maximum M_w, from 3,200 to 11,000. This shows that higher fuel concentrations lead to more-extensive polymerization through increased anhydride bond formation, as expected. The M_w increased further to 16,000 with 2.0 equiv of EDC. Thus, there is a diminishing increase in M_w with higher fuel loadings, consistent with the step-growth mechanism, where M_w is controlled by end-group concentration and undersirable macrocyclization reactions of the growing polymers. Higher fuel concentrations also led to longer-lived polymers. The lifetime τ_{tpl} of the transient polymer increased from ~5 d, to ~7 d, to ~9 d when using 0.5, 1.0, or 2.0 equivalents of EDC. This is most likely due to higher overall conversion and residual EDC enabling the reformation of anhydrides upon hydrolysis.

The fuel concentration had an unexpected impact on the formation of the macrocycle **mC**. As is apparent in Figure 3, higher fuel loadings gave a substantial increase in its production. When employing 0.5 equiv fuel, we observed 40% unreacted **mDA** and 60% of **mP** (M_w = 3,100) after 40 min. There was no significant formation of macrocycle **mC** under these conditions. When increasing the fuel loading to 1.0 equivalents EDC, the percentage of macrocycle increased to 16% at this same time point, while the polymer (M_w = 11,000) was 80%. This trend continued with the use of 2.0 equivalents of EDC, where macrocycle formation further increased to 30% and the polymer (M_w = 14,000) was 64%. That is, with a fuel stoichiometry exceeding 1.0 equiv, longer polymers were synthesized, but the yield of these longer polymers decreased in favor of increased production of macrocycles. It appears that the while the rapid polymerization induced by higher fuel concentrations leads to the creation of long-chain polymers, the rapid reaction and high activation of carboxylic acids also reduces the efficiency of the activated monomer locating the polymer ends, thereby promoting cyclization.

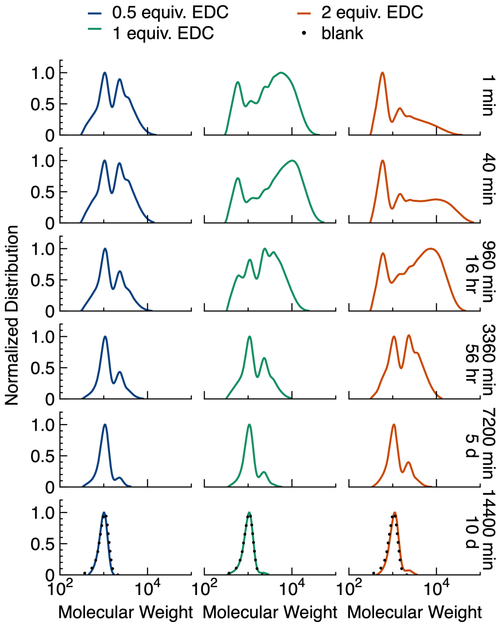

Figure 3: GPC chromatograms for the polymerization of **mDA** with different amounts of fuel at room temperature. Conditions: **mDA** (101 mM), EDC (51 mM), and pyridine (58 mM); **mDA** (101 mM), EDC (102 mM), and pyridine (63 mM); **mDA** (101 mM), EDC (203 mM), and pyridine (66 mM) in 80:20 acetone:water at room temperature.

Figure 4 shows the effect of varying the initial concentration of the monomer. As expected, the peak M_w increases as the concentration of **mDA** is raised from 100 to 200 mM. The maximum M_w for polymer formation observed was 18,000 with $Đ$ of 1.75 for the 200 mM concentration, nearly doubling the value obtained at 100 mM (M_w = 11,000, $Đ$ 1.95). This shows that the higher absolute concentration promotes intermolecular coupling reactions, leading to higher-molecular-weight compounds. The proportion of macrocycle formed is also lower when higher monomer concentration is used, consistent with this assertion. The lifetime τ_{tpl} is essentially unaffected by the concentration of monomer (162 h for 200 mM and 157 h for 100 mM). Thus, despite changes in monomer concentration, the kinetics of polymerization and degradation processes remain consistent with pseudo-first-order hydrolysis.[40]

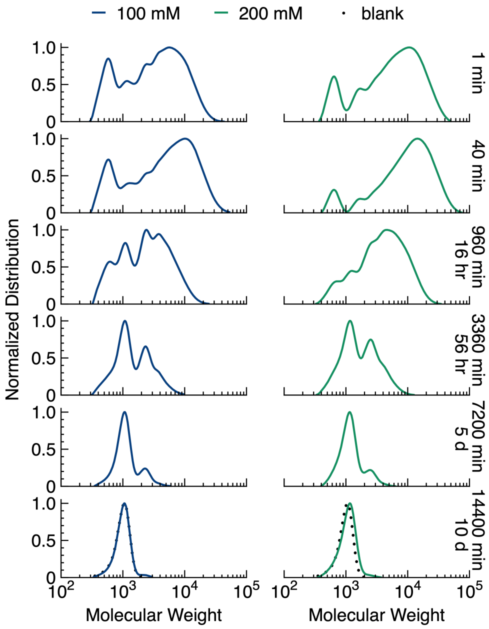

Figure 4: Comparison of different concentrations of **mDA** with one equivalent of EDC. Conditions: **mDA** (101 mM), EDC (102 mM), and pyridine (63 mM); **mDA** (200 mM), EDC (201 mM), and pyridine (63 mM) in 80:20 acetone:water at room temperature.

Considered together, the results show that covalent polymerization is a useful model for studying assembly in nonequilibrium reaction networks. Unlike previous examples,[7,25] the flexibility of monomers **mDA** and **pDA** allows polymerization to outcompete macrocyclization, although macrocycles are still generally observed. Importantly, the relatively slow formation and decomposition of the covalent polymers, compared to analogous transient supramolecular polymers, allows the convenient measure of the degree of the polymerization to quantify each systems' behavior. Variations in the rates of depolymerization highlight that the kinetics of these systems can be controlled over orders of magnitude using well-understood behaviors (e.g., the large difference in τ_{tpl} for **pP** vs **mP**).

Analysis of these systems reveals some important potential features of nonequilibrium polymerization that would be otherwise difficult to detect, such as diminishing yields of longer polymers at higher fuel concentrations because of competing cyclization. In future work, these systems should provide a useful platform for incorporating other elements of kinetic control, such as catalysis, to develop more-sophisticated behavior.

Conclusion

In summary, carbodiimide-driven assembly has allowed us to successfully generate transient aqueous poly(anhydrides). The position of the alkoxy substituent in the monomers, whether *meta* or *para* to the acid group, exerts a significant influence on the lifespan of the polymers, showing that the kinetics of these systems can be controlled. Further, other factors, such as solvent polarity and fuel loading, have significant effects on assembly and disassembly. More-polar solvents and higher carbodiimide concentrations give longer polymer lifespans. Increased monomer concentration also leads to higher molecular weight polymerization, while the kinetics of polymerization and degradation of polymer remain constant. In all cases, the effect of competing macrocyclization must be considered. This work advances the field of fuel-driven assembly by providing a platform to study transient polymers with tunable lifetimes.

Acknowledgements

This work was supported by the United States Department of Energy, Office of Science, Basic Energy Sciences, under Award No. DE-SC0018645. 400 MHz NMR instrumentation at Miami University is supported through funding from the National Science Foundation under Award No. CHE-1919850.

References

(1) Boekhoven, J.; Hendriksen, W. E.; Koper, G. J. M.; Eelkema, R.; van Esch, J. H. Transient Assembly of Active Materials Fueled by a Chemical Reaction. *Science* **2015**, *349* (6252), 1075–1079. https://doi.org/10.1126/science.aac6103.

(2) Sharko, A.; Livitz, D.; De Piccoli, S.; Bishop, K. J. M.; Hermans, T. M. Insights into Chemically Fueled Supramolecular Polymers. *Chem. Rev.* **2022**, *122* (13), 11759–11777. https://doi.org/10.1021/acs.chemrev.1c00958.

(3) Borsley, S.; Leigh, D. A.; Roberts, B. M. W. Chemical Fuels for Molecular Machinery. *Nat. Chem.* **2022**, *14* (7), 728–738. https://doi.org/10.1038/s41557-022-00970-9.

(4) Wilson, M. R.; Solà, J.; Carlone, A.; Goldup, S. M.; Lebrasseur, N.; Leigh, D. A. An Autonomous Chemically Fuelled Small-Molecule Motor. *Nature* **2016**, *534* (7606), 235–240. https://doi.org/10.1038/nature18013.

(5) Erbas-Cakmak, S.; Fielden, S. D. P.; Karaca, U.; Leigh, D. A.; McTernan, C. T.; Tetlow, D. J.; Wilson, M. R. Rotary and Linear Molecular Motors Driven by Pulses of a Chemical Fuel. *Science* **2017**, *358* (6361), 340–343. https://doi.org/10.1126/science.aao1377.

(6) Jalani, K.; Dhiman, S.; Jain, A.; George, S. J. Temporal Switching of an Amphiphilic Self-Assembly by a Chemical Fuel-Driven Conformational Response. *Chem. Sci.* **2017**, *8* (9), 6030–6036. https://doi.org/10.1039/c7sc01730h.

(7) Hossain, M. M.; Atkinson, J. L.; Hartley, C. S. Dissipative Assembly of Macrocycles Comprising Multiple Transient Bonds. *Angew. Chemie - Int. Ed.* **2020**, *59* (33), 13807–13813. https://doi.org/10.1002/anie.202001523.

(8) Borsley, S.; Leigh, D. A.; Roberts, B. M. W.; Vitorica-Yrezabal, I. J. Tuning the Force, Speed, and Efficiency of an Autonomous Chemically Fueled Information Ratchet. *J. Am. Chem. Soc.* **2022**, *144* (37), 17241–17248. https://doi.org/10.1021/jacs.2c07633.

(9) Boekhoven, J.; Brizard, A. M.; Kowlgi, K. N. K.; Koper, G. J. M.; Eelkema, R.; Van Esch, J. H. Dissipative Self-Assembly of a Molecular Gelator by Using a Chemical Fuel. *Angew. Chem. Int. Ed.* **2010**, *49* (28), 4825–4828. https://doi.org/10.1002/anie.201001511.

(10) Tena-Solsona, M.; Rieß, B.; Grötsch, R. K.; Löhrer, F. C.; Wanzke, C.; Käsdorf, B.; Bausch, A. R.; Müller-Buschbaum, P.; Lieleg, O.; Boekhoven, J. Non-Equilibrium Dissipative Supramolecular Materials with a Tunable Lifetime. *Nat. Commun.* **2017**, *8* (May), 1–8. https://doi.org/10.1038/ncomms15895.

(11) Kriebisch, B. A. K.; Jussupow, A.; Bergmann, A. M.; Kohler, F.; Dietz, H.; Kaila, V. R. I.; Boekhoven, J. Reciprocal Coupling in Chemically Fueled Assembly: A Reaction Cycle Regulates Self-Assembly and Vice Versa. *J. Am. Chem. Soc.* **2020**, *142* (49), 20837–20844. https://doi.org/10.1021/jacs.0c10486.

(12) Rodon-Fores, J.; Würbser, M. A.; Kretschmer, M.; Rieß, B.; Bergmann, A. M.; Lieleg, O.; Boekhoven, J. A Chemically Fueled Supramolecular Glue for Self-Healing Gels. *Chem. Sci.* **2022**, *13* (38), 11411–11421. https://doi.org/10.1039/d2sc03691f.

(13) Panja, S.; Fuentes-Caparrós, A. M.; Cross, E. R.; Cavalcanti, L.; Adams, D. J. Annealing Supramolecular Gels by a Reaction Relay. *Chem. Mater.* **2020**, *32* (12), 5264–5271. https://doi.org/10.1021/acs.chemmater.0c01483.

(14) Panja, S.; Patterson, C.; Adams, D. J. Temporally-Programmed Transient Supramolecular Gels. *Macromol. Rapid Commun.* **2019**, *40* (15), 1–6. https://doi.org/10.1002/marc.201900251.

(15) Panja, S.; Dietrich, B.; Adams, D. J. Chemically Fuelled Self-Regulating Gel-to-Gel Transition. *ChemSystemsChem* **2020**, *2* (1), 1–5. https://doi.org/10.1002/syst.201900038.

(16) Biagini, C.; Albano, S.; Caruso, R.; Mandolini, L.; Berrocal, J. A.; Di Stefano, S. Variations in the Fuel Structure Control the Rate of the Back and Forth Motions of a Chemically Fuelled Molecular Switch. *Chem. Sci.* **2018**, *9* (1), 181–188. https://doi.org/10.1039/c7sc04123c.

(17) Bai, S.; Niu, X.; Wang, H.; Wei, L.; Liu, L.; Liu, X.; Eelkema, R.; Guo, X.; van Esch, J. H.; Wang, Y. Chemical Reaction Powered Transient Polymer Hydrogels for Controlled Formation and Free Release of Pharmaceutical Crystals. *Chem. Eng. J.* **2021**, *414* (November 2020), No. 128877. https://doi.org/10.1016/j.cej.2021.128877.

(18) Klemm, B.; Lewis, R. W.; Piergentili, I.; Eelkema, R. Temporally Programmed Polymer – Solvent Interactions Using a Chemical Reaction Network. *Nat. Commun.* **2022**, *13* (1), 1–12. https://doi.org/10.1038/s41467-022-33810-y.

(19) Sun, M.; Deng, J.; Walther, A. Communication and Cross-Regulation between Chemically Fueled Sender and Receiver Reaction Networks**. *Angew. Chem. Int. Ed.* **2023**, *62* (2), e 202214499. https://doi.org/10.1002/anie.202214499.

(20) Rajawasam, C. W. H.; Tran, C.; Weeks, M.; McCoy, K. S.; Ross-Shannon, R.; Dodo, O. J.; Sparks, J. L.; Hartley, C. S.; Konkolewicz, D. Chemically Fueled

Reinforcement of Polymer Hydrogels. *J. Am. Chem. Soc.* **2023**, *145* (9), 5553–5560. https://doi.org/10.1021/jacs.3c00668.

(21) Kariyawasam, L. S.; Hossain, M. M.; Hartley, C. S. The Transient Covalent Bond in Abiotic Nonequilibrium Systems. *Angew. Chem. Int. Ed.* **2021**, *60* (23), 12648–12658. https://doi.org/10.1002/anie.202014678.

(22) Sorrenti, A.; Leira-Iglesias, J.; Sato, A.; Hermans, T. M. Non-Equilibrium Steady States in Supramolecular Polymerization. *Nat. Commun.* **2017**, *8* (May), 1–8. https://doi.org/10.1038/ncomms15899.

(23) Van Ravensteijn, B. G. P.; Hendriksen, W. E.; Eelkema, R.; Van Esch, J. H.; Kegel, W. K. Fuel-Mediated Transient Clustering of Colloidal Building Blocks. *J. Am. Chem. Soc.* **2017**, *139* (29), 9763–9766. https://doi.org/10.1021/jacs.7b03263.

(24) Berrocal, J. A.; Biagini, C.; Mandolini, L.; Di Stefano, S. Coupling of the Decarboxylation of 2-Cyano-2-Phenylpropanoic Acid to Large-Amplitude Motions: A Convenient Fuel for an Acid-Base-Operated Molecular Switch. *Angew. Chem. Int. Ed.* **2016**, *55* (24), 6997–7001. https://doi.org/10.1002/anie.201602594.

(25) Kariyawasam, L. S.; Hartley, C. S. Dissipative Assembly of Aqueous Carboxylic Acid Anhydrides Fueled by Carbodiimides. *J. Am. Chem. Soc.* **2017**, *139* (34), 11949–11955. https://doi.org/10.1021/jacs.7b06099.

(26) Nédélec, F. J.; Surrey, T.; Maggs, A. C.; Leibler, S. Self-Organization of Microtubules and Motors. *Nature* **1997**, *389* (6648), 305–308. https://doi.org/10.1038/38532.

(27) Desai, A.; Mitchison, T. J. Microtubule Polymerization Dynamics. *Annu. Rev. Cell Dev. Biol.* **1997**, *13*, 83–117. https://doi.org/10.1146/annurev.cellbio.13.1.83.

(28) Whitesides, G. M.; Grzybowski, B. Self-Assembly at All Scales. *Science* **2002**, *295* (5564), 2418–2421. https://doi.org/10.1126/science.1070821.

(29) Aprahamian, I.; Goldup, S. M. Non-Equilibrium Steady States in Catalysis, Molecular Motors, and Supramolecular Materials: Why Networks and Language Matter. *J. Am. Chem. Soc.* **2023**, *145* (26), 14169–14183. https://doi.org/10.1021/jacs.2c12665.

(30) Sorrenti, A.; Leira-Iglesias, J.; Markvoort, A. J.; De Greef, T. F. A.; Hermans, T. M. Non-Equilibrium Supramolecular Polymerization. *Chem. Soc. Rev.* **2017**, *46* (18), 5476–5490. https://doi.org/10.1039/c7cs00121e.

(31) Afrose, S. P.; Ghosh, C.; Das, D. Substrate Induced Generation of Transient Self-Assembled Catalytic Systems. *Chem. Sci.* **2021**, *12* (44), 14674–14685. https://doi.org/10.1039/d1sc03492h.

(32) Van Rossum, S. A. P.; Tena-Solsona, M.; Van Esch, J. H.; Eelkema, R.; Boekhoven, J. Dissipative Out-of-Equilibrium Assembly of Man-Made Supramolecular Materials. *Chem. Soc. Rev.* **2017**, *46* (18), 5519–5535. https://doi.org/10.1039/c7cs00246g.

(33) Bal, S.; Das, K.; Ahmed, S.; Das, D. Chemically Fueled Dissipative Self-Assembly That Exploits Cooperative Catalysis. *Angew. Chem. Int. Ed.* **2019**, *58* (1), 244–247. https://doi.org/10.1002/anie.201811749.

(34) Afrose, S. P.; Bal, S.; Chatterjee, A.; Das, K.; Das, D. Designed Negative Feedback from Transiently Formed Catalytic Nanostructures. *Angew. Chem. Int. Ed.* **2019**, *58* (44), 15783–15787. https://doi.org/10.1002/anie.201910280.

(35) Kriebisch, C. M. E.; Bergmann, A. M.; Boekhoven, J. Fuel-Driven Dynamic Combinatorial Libraries. *J. Am. Chem. Soc.* **2021**, *143* (20), 7719–7725. https://doi.org/10.1021/jacs.1c01616.

(36) Kretschmer, M.; Winkeljann, B.; Kriebisch, B. A. K.; Boekhoven, J.; Lieleg, O. Viscoelastic Behavior of Chemically Fueled Supramolecular Hydrogels under Load and Influence of Reaction Side Products. *Commun. Mater.* **2021**, *2* (1), 1–10. https://doi.org/10.1038/s43246-021-00202-6.

(37) Bergmann, A. M.; Bauermann, J.; Bartolucci, G.; Donau, C.; Stasi, M.; Holtmannspötter, A.-L.; Jülicher, F.; Weber, C. A.; Boekhoven, J. Liquid Spherical Shells Are a Non-Equilibrium Steady State. *Commun. Mater* **2021**, *2*, 1–10. https://doi.org/10.1038/s41467-023-42344-w.

(38) Späth, F.; Donau, C.; Bergmann, A. M.; Kränzlein, M.; Synatschke, C. V.; Rieger, B.; Boekhoven, J. Molecular Design of Chemically Fueled Peptide-Polyelectrolyte Coacervate-Based Assemblies. *J. Am. Chem. Soc.* **2021**, *143* (12), 4782–4789. https://doi.org/10.1021/jacs.1c01148.

(39) Wanzke, C.; Jussupow, A.; Kohler, F.; Dietz, H.; Kaila, V. R. I.; Boekhoven, J. Dynamic Vesicles Formed By Dissipative Self-Assembly. *ChemSystemsChem* **2020**, *2* (1), 1–7. https://doi.org/10.1002/syst.201900044.

(40) Zhang, B.; Jayalath, I. M.; Ke, J.; Sparks, J. L.; Hartley, C. S.; Konkolewicz, D. Chemically Fueled Covalent Crosslinking of Polymer Materials. *Chem. Commun.* **2019**, *55* (14), 2086–2089. https://doi.org/10.1039/c8cc09823a.

(41) Würbser, M. A.; Schwarz, P. S.; Heckel, J.; Bergmann, A. M.; Walther, A.; Boekhoven, J. Chemically Fueled Block Copolymer Self-Assembly into Transient Nanoreactors**. *ChemSystemsChem* **2021**, *3* (5), 1–6. https://doi.org/10.1002/syst.202100015.

(42) Chen, X.; Soria-Carrera, H.; Zozulia, O.; Boekhoven, J. Suppressing Catalyst Poisoning in the Carbodiimide-Fueled Reaction Cycle. *Chem. Sci.* **2023**, 12653–12660. https://doi.org/10.1039/d3sc04281b.

(43) The measured difference in M_w between the monomers and macrocycles is outside the typical GPC error of ~10%.

(44) Chen, X.; Soria-Carrera, H.; Zozulia, O.; Boekhoven, J. Suppressing Catalyst Poisoning in the Carbodiimide-Fueled Reaction Cycle. *Chem. Sci.* **2023**, *14* (44), 12653–12660. https://doi.org/10.1039/d3sc04281b.

(45) De Alwis Watuthanthrige, N.; Reeves, J. A.; Dolan, M. T.; Valloppilly, S.; Zanjani, M. B.; Ye, Z.; Konkolewicz, D. Wavelength-Controlled Synthesis and Degradation of Thermoplastic Elastomers Based on Intrinsically Photoresponsive Phenyl Vinyl Ketone. *Macromolecules* **2020**, *53* (13), 5199–5207. https://doi.org/10.1021/acs.macromol.0c00401.

(46) Burridge, K. M.; Parnell, R. F.; Kearns, M. M.; Page, R. C.; Konkolewicz, D. Two-Distinct Polymer Ubiquitin Conjugates by Photochemical Grafting-From. *Macromol. Chem. Phys.* **2021**, *222* (14), 1–9. https://doi.org/10.1002/macp.202100091.

(47) Kromidas, S; Kuss, H. Qualification of GPC/GFC/SEC Data and Results. In *Quantification in LC and GC-A Practical Guide To Good Chromatography Data*; Wiley-VCH Verlag GmbH & Co. KGaA, Weinheim, 2009; pp 271–302.

(48) Hansch, C.; Leo, A.; Taft, R. W. A Survey of Hammett Substituent Constants and

Resonance and Field Parameters. *Chem. Rev.* **1991**, *91* (2), 165–195. https://doi.org/10.1021/cr00002a004.

(49) Kariyawasam, L. S.; Kron, J. C.; Jiang, R.; Sommer, A. J.; Hartley, C. S. Structure-Property Effects in the Generation of Transient Aqueous Benzoic Acid Anhydrides by Carbodiimide Fuels. *J. Org. Chem.* **2020**, *85* (2), 682–690. https://doi.org/10.1021/acs.joc.9b02746.

(50) Berliner, E.; Altschul, L. H. The Hydrolysis of Substituted Benzoic Anhydrides. *J. Am. Chem. Soc.* **1952**, *74* (16), 4110–4113. https://doi.org/10.1021/ja01136a045.

(51) Gold, V. The Hydrolysis of Acetic Anhydride. *Trans. Faraday Soc.* **1948**, *44* (0), 506–518. https://doi.org/10.1039/TF9484400506.

(52) Kirsch, J. F.; Jencks, W. P. Nonlinear Structure-Reactivity Correlations. The Imidazole-Catalyzed Hydrolysis of Esters. *J. Am. Chem. Soc.* **1964**, *86* (5), 837–846. https://doi.org/10.1021/ja01059a019.